Electronic Supplementary Material (ESI) for Journal of Materials Chemistry A.

Supporting Information

Robust three-dimensional carbon conductive network in NaVPO$_4$F cathode towards superior high-rate and ultralong-lifespan sodium-ion full batteries

Chen-De Zhao,[‡a] *Jin-Zhi Guo,*[‡b] *Zhen-Yi Gu,*[b] *Xin-Xin Zhao,*[a] *Wen-Hao Li,*[b] *Xu Yang,*[a] *Hao-Jie Liang*[b] *and Xing-Long Wu*[*ab]

[a] Faculty of Chemistry, National & Local United Engineering Lab for Power Battery, Northeast Normal University, Changchun, Jilin 130024, P. R. China.
[b] Key Laboratory for UV Light-Emitting Materials and Technology, Northeast Normal University, Ministry of Education, Changchun, Jilin 130024, P. R. China.
E-mail: xinglong@nenu.edu.cn

‡ Equal contribution
* The corresponding authors

Experimental Section

Material Synthesis

Preparation of the graphene oxide: The graphene oxide was prepared according to our recent reports.[1]

Preparation of the NVPF@GO cathode: The $NaVPO_4F$ composites coated with reduced graphene oxide (rGO) carbon network were prepared by a two-step solid state carbon thermal reduction (CTR) method. First of all, the V_2O_5, $NH_4H_2PO_4$ and $C_6H_{12}O_6$ raw materials with a molar ratio of 3:6:1 were well mixed by planetary ball milling in ethanol liquid media to synthesize green VPO_4 intermediate precursor ($3\ V_2O_5 + 6\ NH_4H_2PO_4 + C_6H_{12}O_6 = 6\ VPO_4 + 6\ NH_3 + 15\ H_2O + 6\ CO$, the addition of glucose was used as a reducing agent, which reduces V^{5+} to V^{3+}). The as-prepared mixture was dried at 50°C by a rotary evaporator and then heated at 750°C for 8 h under argon atmosphere with a temperature ramp rate of 5°C min^{-1} to obtain the VPO_4 powder product. Secondly, NVPF@5%rGO composites were synthesized with NaF, VPO_4 and graphene oxide with a mass ratio of 1:1:0.1 ($NaF + VPO_4 = NaVPO_4F$, the amount of graphene oxide controls the morphology of carbon framework and the carbon contents in the final products). The ball milling and drying process were the same as the previous step. Then, the mixtures were calcinated at 750°C for 6 h under argon with a heating rate of 5°C min^{-1}. After cooling down completely to room temperature, the black final products were obtained. For comparison, samples without addition and addition of different amounts of graphene oxide were also prepared and marked as NVPF, NVPF@2.5%rGO and NVPF@7.5%rGO. In addition, a series of rGO carbon networks were prepared by dissolving ~5 mg sample powders in 5 ml nitric acid under continuous stirring at 70 °C for 2 h. After natural cooling to room temperature, the obtained solutions were treated with the ultrasound for 30 mins, then, few drops of solutions were transferred on to the silicon slice, and dried in a vacuum oven at 60 °C overnight for scanning electron microscopy (SEM) studies.

Preparation of the hard carbon cloth anode derived from cotton cloth: The hard carbon anode derived from cotton cloth (abbreviated as HC) was prepared according to our recent reports,[2, 3] of which the areal density is about 4.5 mg cm^{-2}.

Material Characterizations

Powder X-ray diffraction (PXRD) patterns of the power samples were collected on Bruker D8 ADVANCE diffractometer with Cu Kα radiation (λ = 0.15406 nm). The experiments were carried out at room temperature with a scan rate of 20° min^{-1} from a 2θ angle of 10° to 60°. And the LeBail fitting is conducted on the high quality PXRD data with the scan rate of 0.02° min^{-1} from a 2θ angle of 10° to 80° using the FullProf Suite software. X-ray photoelectron spectroscopy (XPS) data were obtained by ESCALab220i-XL electron spectrometer from VG Scientific using 300 W Al K α radiation. Fourier transform infrared spectroscopy (FTIR) measurements were implemented on a Nicolet 6700 spectrometer (Thermo). Raman spectra were performed with a confocal Raman microscope (JYHR-800 Lab Ram) in a backscattering configuration with a 488 nm argon ion for excitation. The morphology, composition and particle size of each sample were investigated by using SEM (Hitachi SU8000) and transmission electron microscope (TEM, JEOL-2100F, 200 kV). And the carbon content of in the 3D carbon network constructed $NaVPO_4F$ was measured by CHN Elemental analyzer (Eurovector-EA3000).

Electrochemical measurements

The electrochemical properties were measured in CR2032 coin cells. The cathode electrode consisted of the active material, carbon black, and binder (carboxymethylcellulose) were mixed in deionized water and covered on an aluminium foil in the ratio of 7:2:1 in weight percent. Then, the electrode was dried in a vacuum oven at 60 °C overnight. The loading mass of active material on work electrodes is about 0.8-1.5 mg cm^{-2}. Metallic sodium plate was used as both counter and reference electrodes, and glass microfiber filter (Whatman) was used as the separator. The electrolyte was 1mol L^{-1} $NaClO_4$ dissolved in ethylene carbonate (EC) and propylene carbonate (PC, co-solvent, which could reduce the melting point of EC and increase ionic conductivity of electrolyte) (1:1 in v/v) with 5 vol % fluoroethylene carbonate (FEC, SEI additive, which could reduce solvent decomposition, form the stable passivation layer and suppress the side reactions of sodium metal anode) as the additive. The galvanostatic discharge/charge properties at various current densities were obtained on the battery-testing systems (NEWARE CT-4000) between 2.0 and 4.2 V. Cyclic voltammetry (CV) measurements were performed on a VersaSTAT 3 (Princeton Applied Research) electrochemical workstation over the potential range of 2.0−4.2 V. The electrochemical impedance spectroscopy (EIS) measurements were implemented by using a PARSTAT 4000 (Princeton Applied Research) with the frequency ranging from 10 mHz to 1 MHz with an alternating current amplitude of 5 mV. For galvanostatic intermittent titration technique (GITT) analyses, the cells were cycled in the potential window of 2.0-4.2 V at a rate of 0.1 C. The duration time for each applied galvanostatic current and rest was 25 min and 4 hours, respectively. And the electric conductivity was implemented by conductivity meter (ST2643).

Full cells were fabricated in the glove box by coupling the NVPF@5%rGO cathode with HC anode, and the electrochemical properties were evaluated on the battery testing systems in the voltage window of 2.0-4.2 V. Specific capacities of full-cells were calculated according to the mass of cathode materials. Prior to the fabrication of full cells, pre-sodiation for the HC anodes was employed to activate the material and stabilize the electrode surface before the assembling of HC//NVPF@5%rGO full-cells.

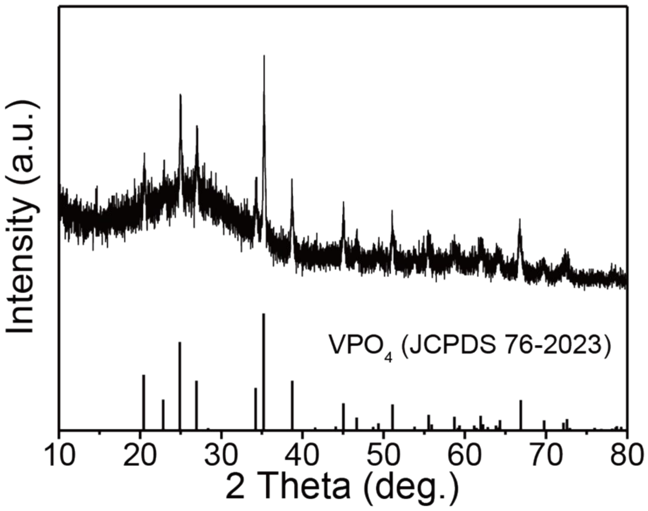

Fig. S1 The XRD pattern of VPO_4 precursor.

All the diffraction peaks of VPO_4 precursor are in good accordance with an orthorhombic crystal phase of VPO_4 (JCPDS Card No. 70-2023).

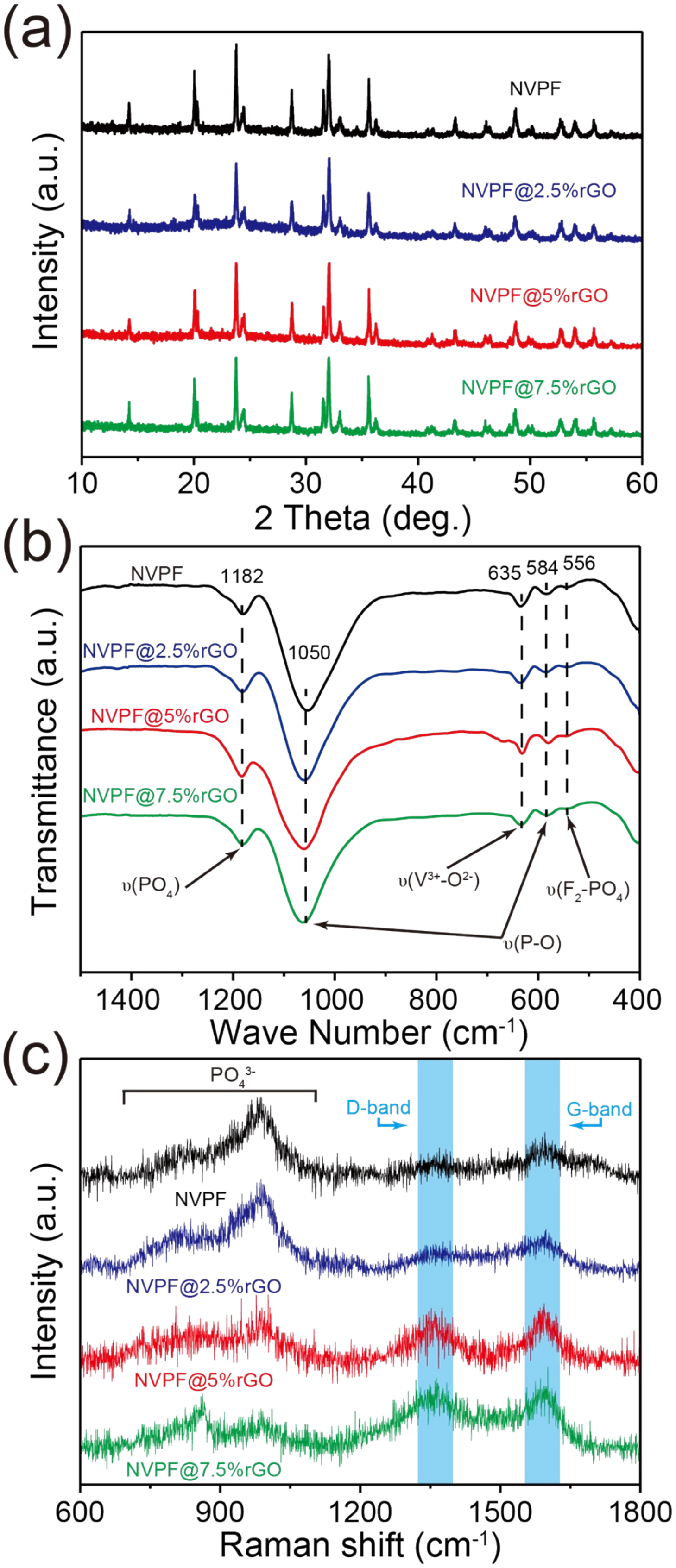

Fig. S2 (a) XRD patterns, (b) FTIR spectra and (c) Raman spectra of the NVPF-based samples.

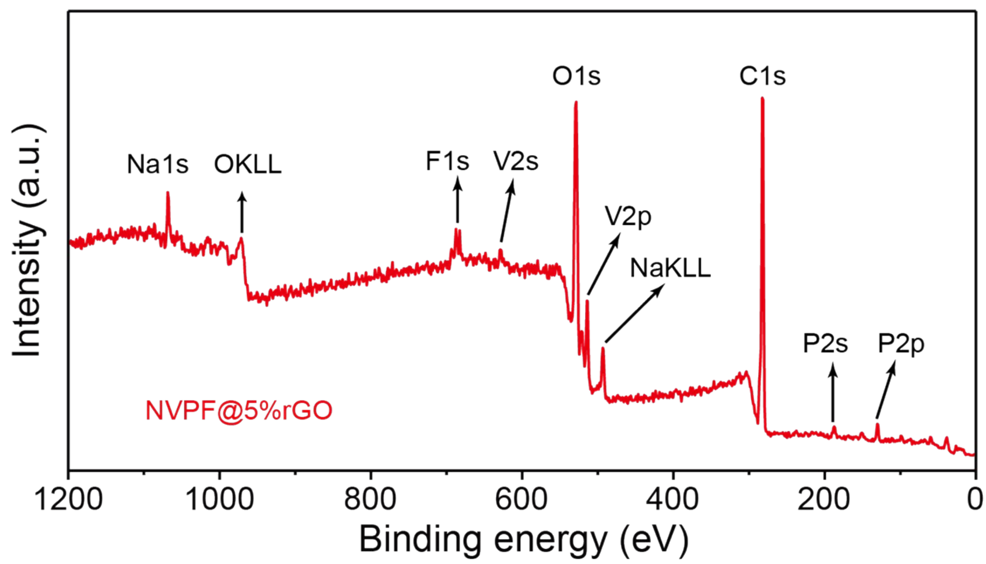

Fig. S3 XPS survey spectrum of NVPF@5%rGO.

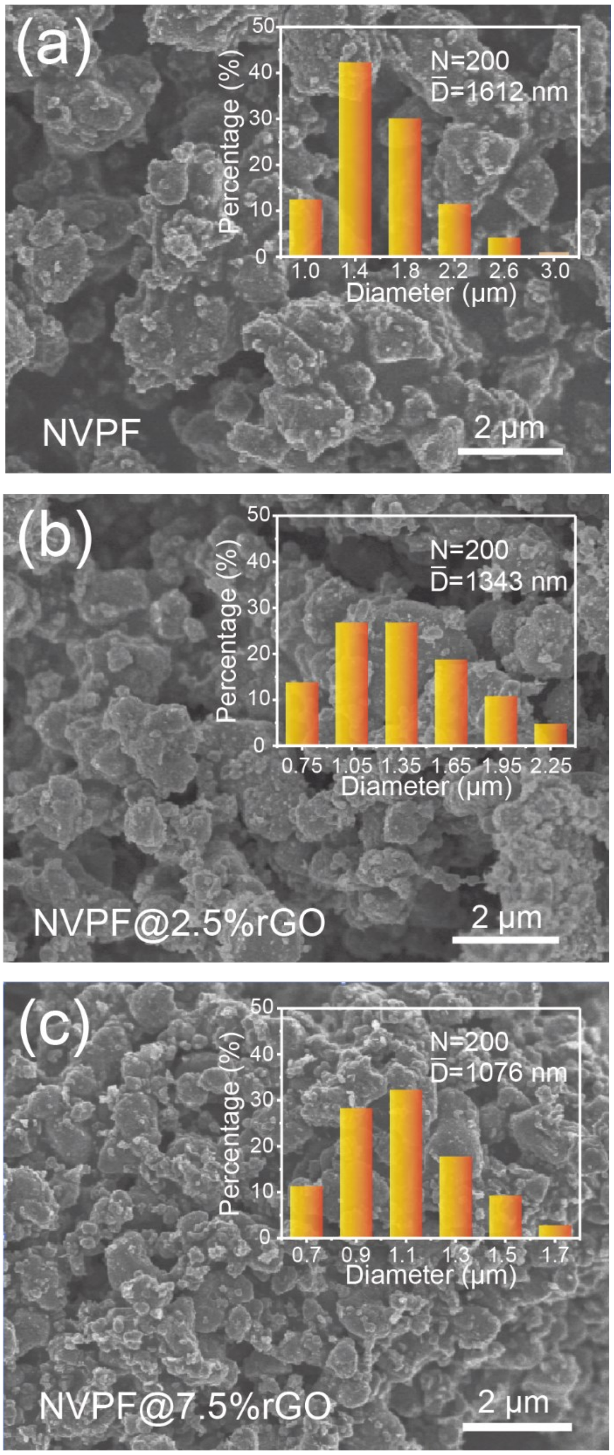

Fig. S4 (a-c) SEM images of the NVPF-based samples.

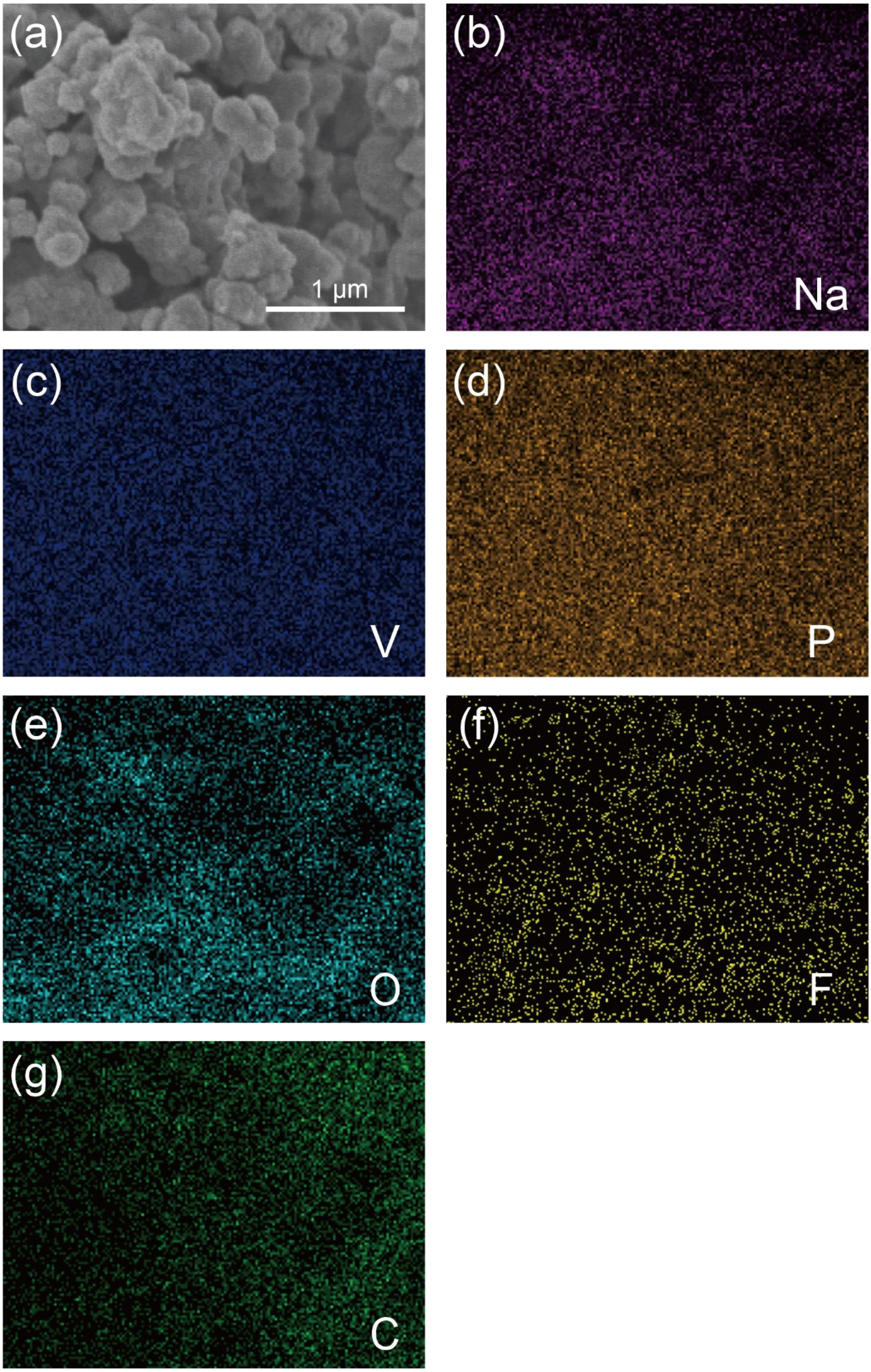

Fig. S5 (a) SEM image and (b-g) elemental mappings of NVPF@5%rGO.

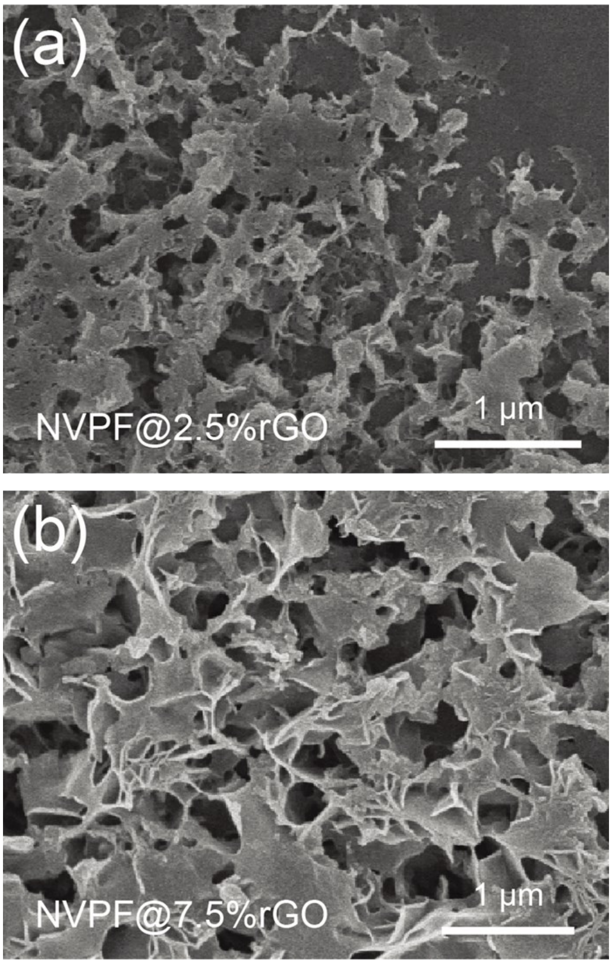

Fig. S6 Carbon network images of (a) NVPF@2.5%rGO and (b) NVPF@7.5%rGO.

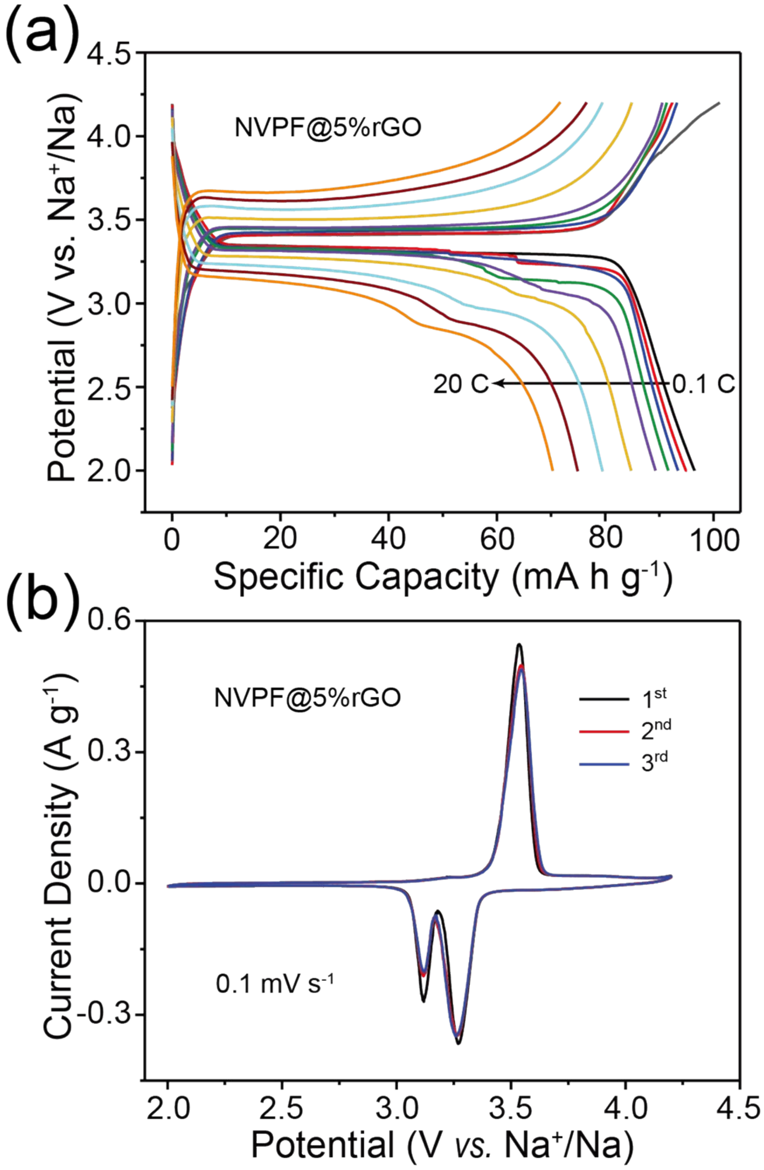

Fig. S7 (a) The GCD profiles at the rate of 0.1-20 C , and (b) CV curves of the initial three cycles at 0.1 mV s^{-1} of NVPF@5%rGO.

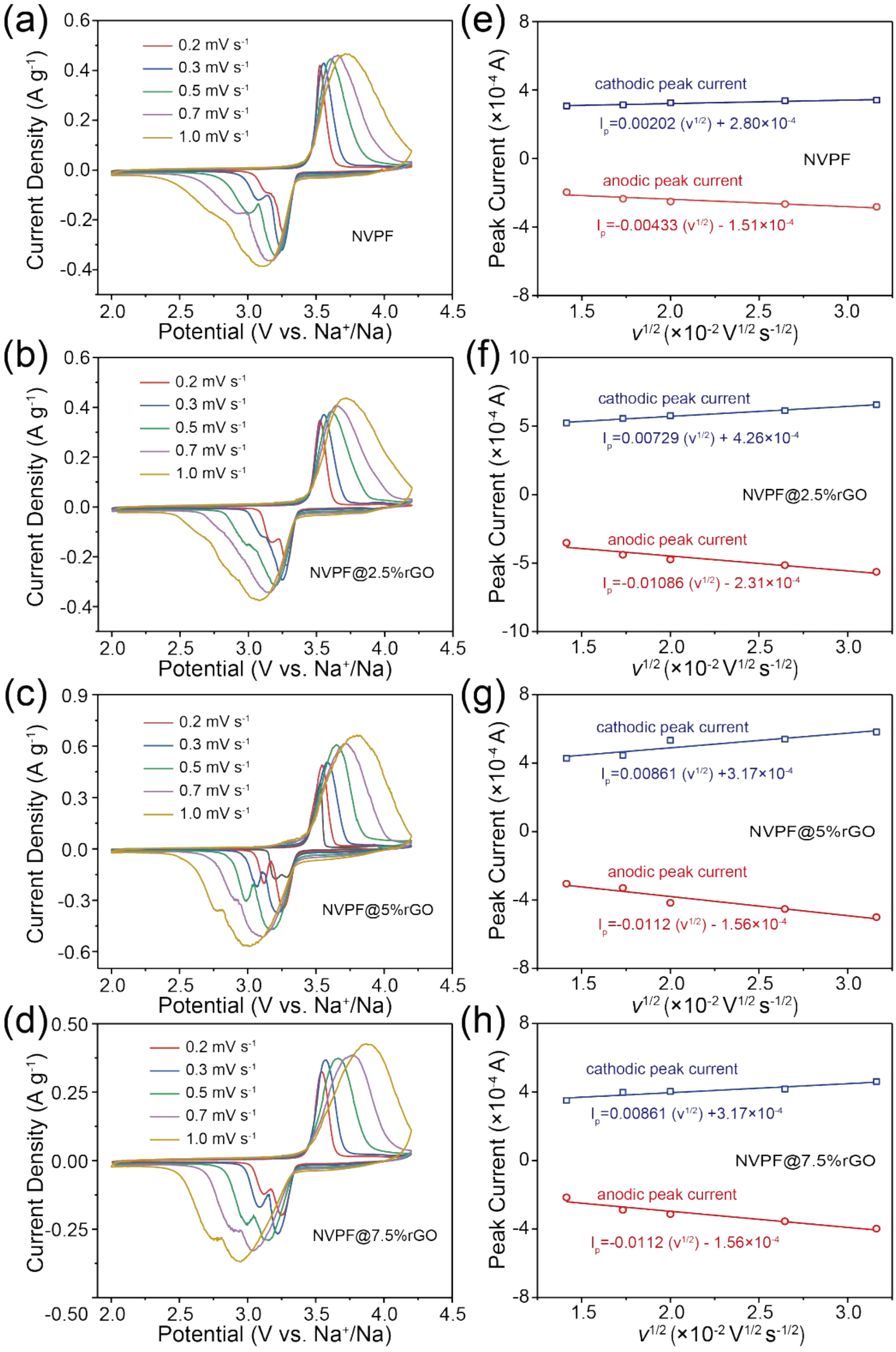

Fig. S8 (a-d) CV profiles at various scan rates from 0.2 to 1.0 mV s^{-1}. (e-h) Linear fitting for the relationship between i_p and $v^{1/2}$ from CV profiles.

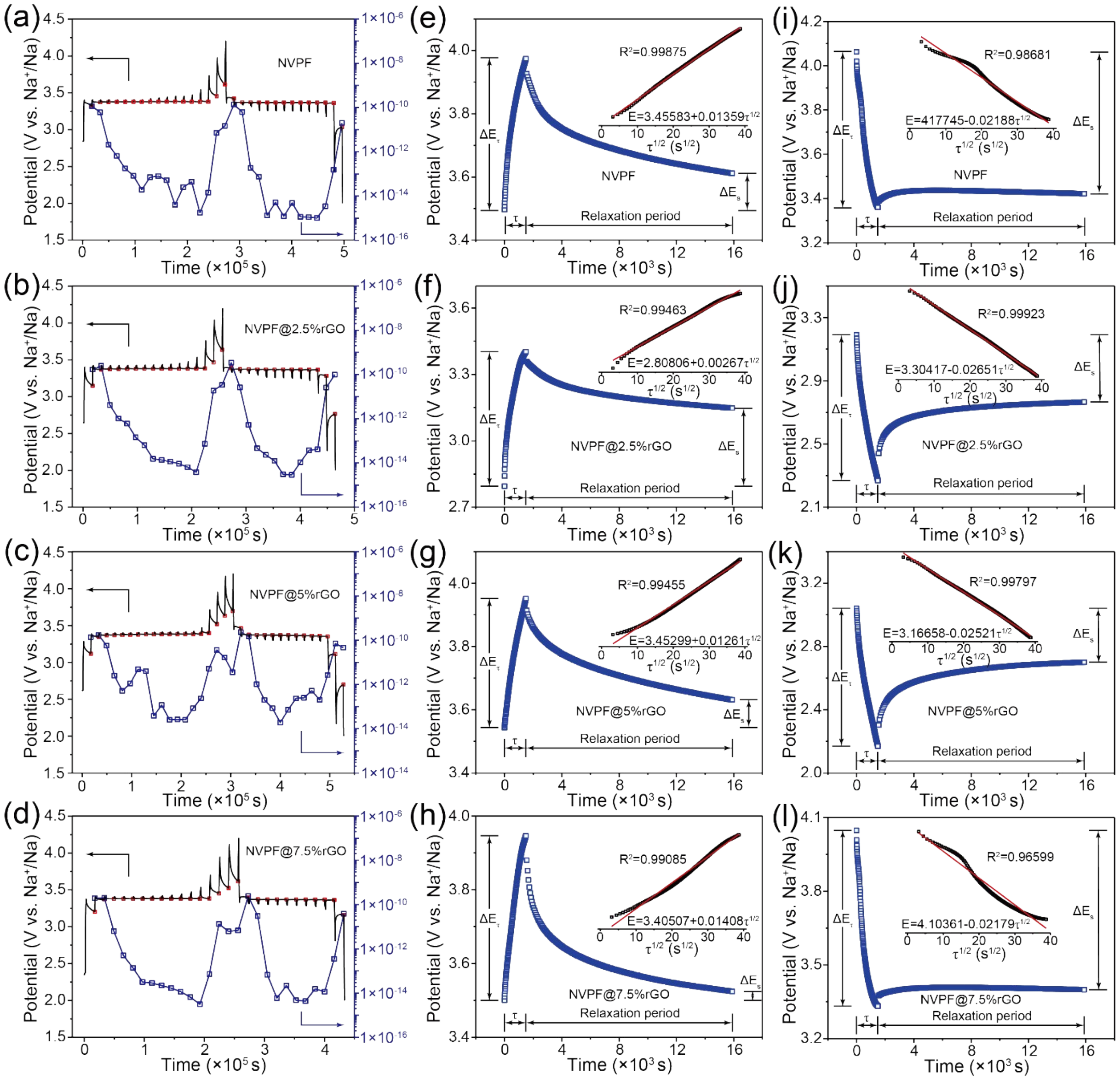

Fig. S9 GITT test results showing the changes of $D_{\mathrm{app,Na}}$ and quasi-equilibrium potentials along with the GCD processes (a-d). The τ vs. E profiles for a single GITT titration during (e-h) charge and (i-l) discharge processes. The corresponding linearly fitting behavior of E vs. $\tau^{1/2}$ for the (inset e-h) charge and (inset i-l) discharge GITT titration.

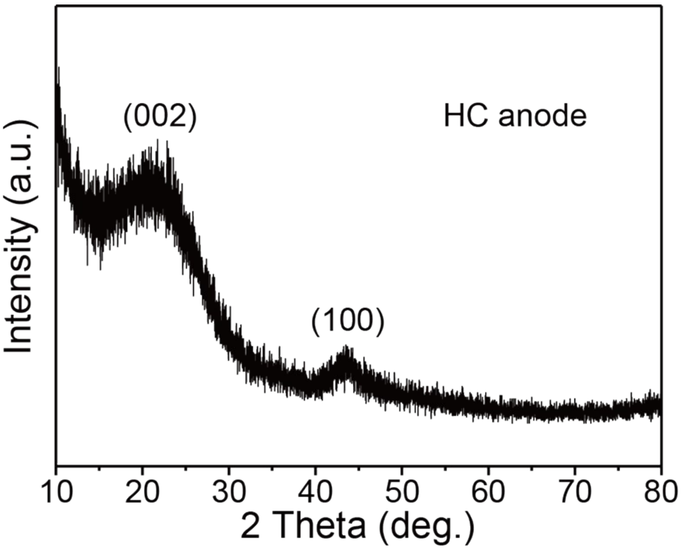

Fig. S10 The XRD pattern of HC anode.

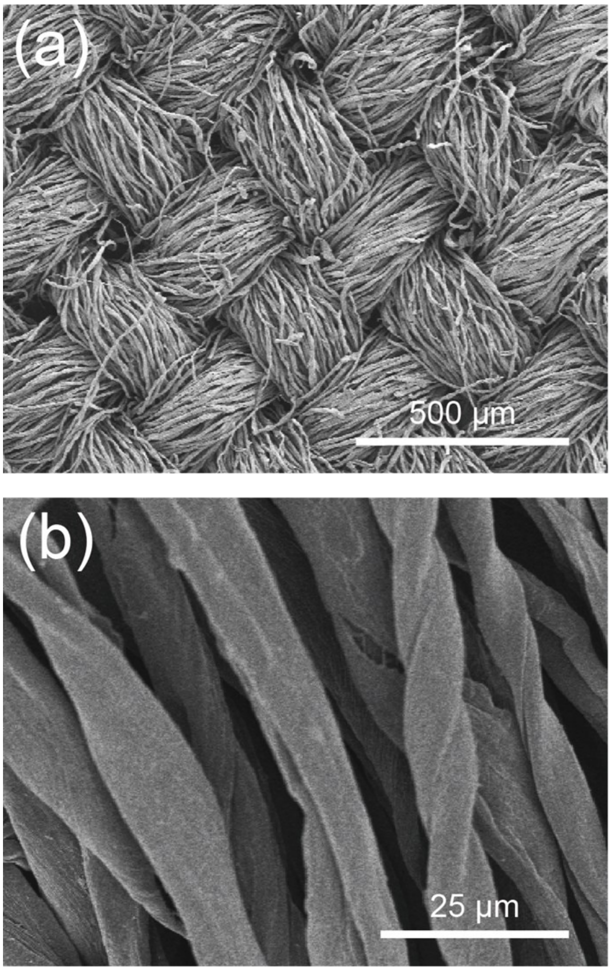

Fig. S11 The SEM images of HC anode.

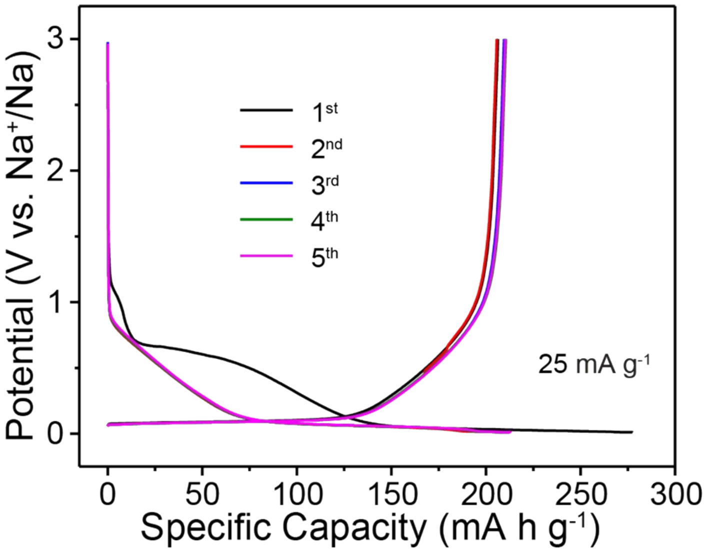

Fig. S12 The GCD curves of HC anode at 25 mA g^{-1} in inital five cycles.

Table S1 The elemental analysis result of NVPF@5%rGO.

Element	% C	% N	% H
NVPF@5%rGO	3.08	0.10	0.06

Calculation process for the apparent Na chemical diffusion coefficients through CV tests

CV curves were recorded in a potential window of 2.0-4.2 V versus Na^+/Na at various scan rates from 0.1 to 1.0 mV s^{-1}. In the CV curves, the $D_{app,Na}$ values were calculated according to the following Randles-Sevcik equation:[3-5]

$$i_p = 2.69 \times 10^5 \, n^{3/2} A \, D_{app,Na}{}^{1/2} C_0 v^{1/2}$$

where i_p is the peak current density, n is the electron-transfer number per molecule formula during the redox reaction (n = 1 for the present NVPF),[6] A is the surface area of the electrode, C_0 is the concentration of Na ions in the electrode (4.675 mmol cm^{-3}),[6] and v is the scan rate.

Calculation process for the apparent Na chemical diffusion coefficients through GITT tests

The $D_{app,Na}$ values can be calculated according to the following equation: [7]

$$D_{app,Na} = \frac{4}{\pi\tau}\left(\frac{m_B V_M}{M_B S}\right)^2 \left(\frac{\Delta E_s}{\Delta E_\tau}\right)^2 \qquad (\tau \ll L^2/D)$$

where m_B, M_B,and V_M are the mass, molecular weight, and molar volume of the NVPF material, respectively; τ is the time for an applied galvanostatic current; S is the active surface of the electrode; L is the average radius of the material particles; and ΔE_s and ΔE_τ are the quasi-equilibrium potential and the change of cell voltage E during the current pulse, respectively.

References

1. F. Wan, J.-Z. Guo, X.-H. Zhang, J.-P. Zhang, H.-Z. Sun, Q. Yan, D.-X. Han, L. Niu and X.-L. Wu, *Acs Appl. Mater. Interfaces*, 2016, **8**, 7790-7799.
2. J.-Z. Guo, Z.-Y. Gu, X.-X. Zhao, M.-Y. Wang, X. Yang, Y. Yang, W.-H. Li and X.-L. Wu, *Adv. Energy Mater.*, 2019, **9**, 1902056.
3. Z.-Y. Gu, J.-Z. Guo, Z.-H. Sun, X.-X. Zhao, W.-H. Li, X. Yang, H.-J. Liang, C.-D. Zhao and X.-L. Wu, *Sci. Bull.*, 2020, **65**, 702-710.
4. Z. Y. Gu, J. Z. Guo, Y. Yang, H. Y. Yu, X. T. Xi, X. X. Zhao, H. Y. Guan, X. Y. He and X. L. Wu, *Inorg. Chem. Front.*, 2019, **6**, 988-995.
5. J.-Z. Guo, P.-F. Wang, X.-L. Wu, X.-H. Zhang, Q. Yan, H. Chen, J.-P. Zhang and Y.-G. Guo, *Adv. Mater.*, 2017, **29**, 1701968.
6. P. Feng, W. Wang, J. Hou, K. Wang, S. Cheng and K. Jiang, *Chem. Eng. J*, 2018, **353**, 25-33.
7. X.-H. Zhang, W.-L. Pang, F. Wan, J.-Z. Guo, H.-Y. Lü, J.-Y. Li, Y.-M. Xing, J.-P. Zhang and X.-L. Wu, *ACS Appl. Mater. Interfaces*, 2016, **8**, 20650-20659.